NAVAL POSTGRADUATE SCHOOL

MONTEREY, CALIFORNIA

THESIS

IDENTIFYING SEDIMENT TRANSPORT POTENTIAL AND VELOCITY PROFILES IN THE CARMEL RIVER USING AN ADP

by

Tyonna N. McPherson

December 2020

Thesis Advisor:	Mara S. Orescanin
Second Reader:	Jeffrey D. Paduan

THIS PAGE INTENTIONALLY LEFT BLANK

REPORT DOCUMENTATION PAGE	*Form Approved OMB No. 0704-0188*

1. AGENCY USE ONLY *(Leave blank)*	**2. REPORT DATE** December 2020	**3. REPORT TYPE AND DATES COVERED** Master's thesis

4. TITLE AND SUBTITLE
IDENTIFYING SEDIMENT TRANSPORT POTENTIAL AND VELOCITY PROFILES IN THE CARMEL RIVER USING AN ADP

5. FUNDING NUMBERS

6. AUTHOR(S) Tyonna N. McPherson

7. PERFORMING ORGANIZATION NAME(S) AND ADDRESS(ES)
Naval Postgraduate School
Monterey, CA 93943-5000

8. PERFORMING ORGANIZATION REPORT NUMBER

9. SPONSORING / MONITORING AGENCY NAME(S) AND ADDRESS(ES)
N/A

10. SPONSORING / MONITORING AGENCY REPORT NUMBER

11. SUPPLEMENTARY NOTES The views expressed in this thesis are those of the author and do not reflect the official policy or position of the Department of Defense or the U.S. Government.

12a. DISTRIBUTION / AVAILABILITY STATEMENT
Approved for public release. Distribution is unlimited.

12b. DISTRIBUTION CODE
A

13. ABSTRACT (maximum 200 words)

The Carmel River runs 58 km from the Santa Lucia Mountains through the Carmel Valley, eventually stopping at a lagoon on Carmel River State Beach. During the winter months, the river breaches through the lagoon, allowing water to freely flow between the river and Carmel Bay. Sediment transport, in part owing to turbulent river discharge and in part owing to ocean forcing (tides and waves), contributes heavily to whether the lagoon is open or closed: when there are low flow conditions, waves and tides can decrease flow rates in the breach, allowing sediment to settle. The sediment budget is expected to be a closed system, owing to the rocky headlands and long-term stability (no yearly regression or transgression) of the shoreline. However, it is currently unknown 1) how velocity profiles evolve during breaching phases, and 2) how much sediment moves during such an event. The hypothesis is that the breach mouth can completely disappear and re-emerge over a single breach-closure cycle. This study uses the RiverSurveyor M9 acoustic Doppler profiler to measure outflow discharge and GPS surveys to quantify elevation changes. A velocity profile can be built that would estimate the sediment transport potential within the breach. The information obtained will help identify and better understand the velocity thresholds that contribute to breaching seasons as well as estimates of sediment transport rates during breaching, which are currently unknown.

14. SUBJECT TERMS Carmel River, acoustic Doppler profiler, ADP, sediment transport, velocity profiles	**15. NUMBER OF PAGES** 53
	16. PRICE CODE

17. SECURITY CLASSIFICATION OF REPORT	**18. SECURITY CLASSIFICATION OF THIS PAGE**	**19. SECURITY CLASSIFICATION OF ABSTRACT**	**20. LIMITATION OF ABSTRACT**
Unclassified	Unclassified	Unclassified	UU

NSN 7540-01-280-5500 Standard Form 298 (Rev. 2-89)
Prescribed by ANSI Std. 239-18

THIS PAGE INTENTIONALLY LEFT BLANK

Approved for public release. Distribution is unlimited.

IDENTIFYING SEDIMENT TRANSPORT POTENTIAL AND VELOCITY PROFILES IN THE CARMEL RIVER USING AN ADP

Tyonna N. McPherson
Lieutenant Commander, United States Navy
BA, University of San Diego, 2009

Submitted in partial fulfillment of the
requirements for the degree of

MASTER OF SCIENCE IN METEOROLOGY AND PHYSICAL OCEANOGRAPHY

from the

NAVAL POSTGRADUATE SCHOOL
December 2020

Approved by: Mara S. Orescanin
Advisor

Jeffrey D. Paduan
Second Reader

Peter C. Chu
Chair, Department of Oceanography

THIS PAGE INTENTIONALLY LEFT BLANK

ABSTRACT

The Carmel River runs 58 km from the Santa Lucia Mountains through the Carmel Valley, eventually stopping at a lagoon on Carmel River State Beach. During the winter months, the river breaches through the lagoon, allowing water to freely flow between the river and Carmel Bay. Sediment transport, in part owing to turbulent river discharge and in part owing to ocean forcing (tides and waves), contributes heavily to whether the lagoon is open or closed: when there are low flow conditions, waves and tides can decrease flow rates in the breach, allowing sediment to settle. The sediment budget is expected to be a closed system, owing to the rocky headlands and long-term stability (no yearly regression or transgression) of the shoreline. However, it is currently unknown 1) how velocity profiles evolve during breaching phases, and 2) how much sediment moves during such an event. The hypothesis is that the breach mouth can completely disappear and re-emerge over a single breach-closure cycle. This study uses the RiverSurveyor M9 acoustic Doppler profiler to measure outflow discharge and GPS surveys to quantify elevation changes. A velocity profile can be built that would estimate the sediment transport potential within the breach. The information obtained will help identify and better understand the velocity thresholds that contribute to breaching seasons as well as estimates of sediment transport rates during breaching, which are currently unknown.

THIS PAGE INTENTIONALLY LEFT BLANK

TABLE OF CONTENTS

I. MOTIVATION 1

II. INTRODUCTION 3

III. METHODOLOGY 7
- **A. FIELDWORK AND DATA COLLECTION 7**
- **B. DATA ANALYSIS 9**
  - **1. River Surveyor 9**
  - **2. GPS Surveys 11**

IV. RESULTS 13
- **A. BREACHING AND CLOSING EVENTS 13**
- **B. ELEVATION TRANSFORMATIONS 15**
  - **1. Longshore 19**
  - **2. Cross-Shore 23**
- **C. EMPIRICAL BERM HEIGHT ESTIMATES 25**
- **D. BREACH VELOCITY PROFILES 26**

V. DISCUSSION 29
- **A. SEDIMENT MOVEMENT AND BERM STABILITY 29**
- **B. RIVER DISCHARGE VS. TIDAL AND WAVE ENERGY 30**

VI. CONCLUSION 31

LIST OF REFERENCES 33

INITIAL DISTRIBUTION LIST 35

THIS PAGE INTENTIONALLY LEFT BLANK

LIST OF FIGURES

Figure 1. Carmel River Breach February 7, 2020 5

Figure 2. Carmel River State Beach Aerial View 6

Figure 3. SonTek RiverSurveyor M9 Acoustic Doppler Profiler 7

Figure 4. ADP Transects 8

Figure 5. GNSS Receiver and GPS Walking Survey Paths 9

Figure 6. Cross Section of ADP Data Collection Transect Area. Adapted from SonTek, a Xylem, brand RiverSurveyor S5/M9 System Manual. 10

Figure 7. RiverSurveyor SmarPulse™ adjustable cells. Source: SonTek, a Xylem, brand RiverSurveyor S5/M9 System Manual. 10

Figure 8. Carmel River State Beach Momentum Balance for Breach/Closure 14

Figure 9. Elevation Plots of Carmel River State Beach Surveys 17

Figure 10. Elevation Difference Plots of Carmel River State Beach Survey 18

Figure 11. Longshore and Cross-Shore Sampling Schematic. 19

Figure 12. Longshore and Cross-Shore Survey Samples 21

Figure 13. Longshore Minimums 22

Figure 14. Lagoon Water Levels, In-Channel Maximums, and Swart Model Berm Estimate 25

Figure 15. ADP Velocity Measurements during the March 5 Breach 27

Figure 16. Upstream Measurement of Carmel River 28

THIS PAGE INTENTIONALLY LEFT BLANK

LIST OF TABLES

Table 1. Carmel River Breach and Closure Dates 15

Table 2. Carmel River Discharge March 5, 2020 28

THIS PAGE INTENTIONALLY LEFT BLANK

LIST OF ACRONYMS AND ABBREVIATIONS

ADP	acoustic Doppler profiler
GLONASS	Global Navigation Satellite System (Russian)
GNSS	Global Navigation Satellite Systems (U.S.)
GPS	Global Positioning System
MHz	megahertz
NAVD88	North American Vertical Datum of 1988 Quasi-
QZSS	Zenith Satellite System
RTK	real-time kinematic
SBAS	Satellite-Based Augmentation System Universal
UTM	Transverse Mercator
WGS84	World Geodetic System 1984

THIS PAGE INTENTIONALLY LEFT BLANK

ACKNOWLEDGMENTS

First, I'd like to thank Dr. Mara Orescanin for the opportunity to work and learn from her. This has been the learning experience of a lifetime. Her guidance and support have made this that much more rewarding and fulfilling. To my Second Reader, Dr. Jeffrey Paduan, thank you for your input and guidance. Mr. Paul Jessen, my "MATLAB Guru," you truly are amazing. To the faculty at NPS as well as my cohort: I've learned so much from all of you and couldn't ask for a better group of Naval Officers and civilians to share this journey with. I thank my parents and siblings, Karen, Darryl, Dominique, and Nyeshia Lewis, for being my ground and foundation. Last, but certainly not least, thanks to my husband, Anthony, and children, Sienna and Jaylen. Thank you for supporting me in everything I do. I am truly blessed to have you.

THIS PAGE INTENTIONALLY LEFT BLANK

I. MOTIVATION

Beach evolution is constant. On any given beach there are numerous environmental factors that contribute to sediment accretion and erosion and develop berm crest elevation and steepness throughout the beach. For ephemeral rivers and estuaries, the factors are coming from both the river and ocean side, which eventually cause a breakdown of the beach head resulting in a breach of the river. During these morphological catastrophes, sediment is forcefully transported and redeposited, in some instances, mere meters from its original placement, in others 10s of meters away. An overall morph can happen in minutes to hours. Given a closed sediment budget, the same sediment migrates along the beach creating features that trigger potential dangers such as flooding or navigational hazards.

Amphibious beach landings are heavily relied upon and widely utilized in Navy and Marine Corps mission sets. Knowing and understanding the dynamics of beach morphology and the possible rate of change is key to mission execution and allows a better understanding for equipment capabilities and limitations.

This study focuses on developing an understanding of the morphological rate of change at Carmel River State Beach, a seasonal ephemeral in Central California. Having models available for beaches that mimic possible operational environments and that accurately predict how a beach will morph based on evolving environmental factors will allow operational flexibility and facilitate increased battle space awareness.

THIS PAGE INTENTIONALLY LEFT BLANK

II. INTRODUCTION

Coastal ephemeral rivers are lagoon systems (also called bar-built estuaries) that periodically open and close allowing an intermittent connection between the ocean and river, through a process called beach breaching. Breaching at a system could be a regularly occurring phenomenon, which transitions with the seasons, or it could be more irregular and relatively unpredictably linked to morphodynamical feedback effects (Davidson et al. 2008, Behrens 2013). The morphological evolution of these rivers is driven by the infilling and backfilling of sediment as well as hydrodynamic forcing from the ocean and river (Rich and Keller 2013). Exact timing of breaching is challenging to predict, making observations of breach morphodynamics sparse.

Forcing from the ocean side, wave energy can erode the face of the beach contributing to the destruction of the sand bar blocking the inlet river channel on the ocean side (Williams 2015). Waves also play a constructive role, however, through wave overtopping, where wave-carried sediment deposits on the beach crest and onto the back of the beach (Donnelly 2008, Laudier et al 2011, Williams, 2015). Assuming berm height is solely dependent on the height at which waves can transport sediment, berm crests can be estimated using parametric berm heigh models such as the Swart 1974 to predict upper beach profile limits (Swart 1974, Booysen, 2017).

Forcing from the land side, river discharge influences the system by increasing water levels within the lagoon and transporting sediment from upstream. When the system is closed, lagoon water levels can increase to the sand bar elevation, which starts a breach through lagoon overtopping and links the estuary and ocean (Pierce 1970, Orescanin and Scooler 2018). River discharge is the result of hydrological processes in a river system, which transport runoff from rainfall. Accumulation in the watershed leads to immense volumes of water flowing down the river during and after high precipitation events.

Water flow in rivers is not uniform at all locations leading to differences in sediment movement. During low or moderate water discharge, sediment mobility is insignificant or not observed. The largest transport of sediment is seen during high velocity

water flow. The flow at a river outlet typically decreases relative to upstream flow enabling pooling downstream, which gives way to lagoon creation in the “backwater” segment of the river (Nittrouer et al. 2012). Increased watershed area along riverbanks positively affects river flow speeds. In the Carmel River, rainfall intensity and distribution, soil moisture conditions, and ground water storage at the Carmel Valley Alluvial Aquifer all factor into whether river flow will advance to the lagoon (James 2005). Increased upstream water demands throughout the years have contributed to the varying stream movement (Kraus and Munger 2008). This makes it harder to predict downstream behaviors as they pertain to downstream ephemerality factors.

The pressure gradient between the ocean and river lagoon dictates constructive and destructive behavior of a bar-built estuary such as Carmel River Lagoon (Orescanin and Scooler 2018). Ocean-side wave overtopping and high tides builds the sand bar separating the ocean from the lagoon and also spills water into the lagoon (Laudier et all 2011). Based on the offshore pressure, the expected build up can be modeled and an approximate elevation can be predicted for the upper beach profile limits (Swart 1974, Booysen 2017).

While lagoon water levels rise as river discharge increases, lagoon-side seepage and liquefaction give way to sediment mobility (Figure 1). On the California coast the lagoon-side openings occur after a rainy season increases river water levels and discharge rates (Kraus and Wamsley 2003). Thresholds outlined in a previous study by the Monterey Peninsula Water Management District (MPWMD) conclude that lagoon inflow rates of 100–200 ft^3/s will maintain an open lagoon and below 10 ft^3/s the mouth will stay closed (James 2005). Lagoon water level thresholds vary with each breach as the gradient is largely dependent on the beach elevation (Orescanin and Scooler 2018).

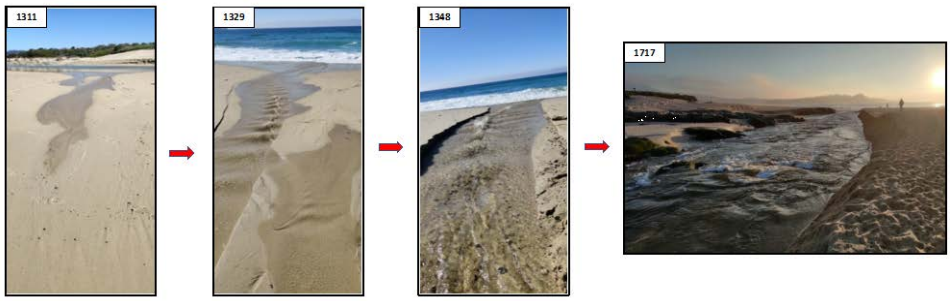

Photographs were taking during various stages of a breach between the river lagoon and the Carmel Bay at Carmel River State Beach. The photograph at 1311was taken facing the lagoon while the photographs at 1329,1348, and 1717 were taken facing the Carmel Bay and Pacific Ocean.

Figure 1. Carmel River Breach February 7, 2020

When ocean forcing is stronger than lagoon forcing, the sediment becomes a part of the sandbar that blocks the river mouth (Orescanin and Scooler 2018). The morphology of the barrier beach area in part is determined by the pressure gradient created between the ocean wave forced sediment and the river transported sediment, the ocean wave constructive process and the river flow destructive process (FitzGerald 1996, Behrens et al. 2013, Orescanin and Scooler 2018). In northern California, ephemeral rivers tend to breach from the lagoon side owing to the increased water-head pressure and increased lagoon water levels (Kraus and Munger 2008).

Long-term channel morphology can be predicted by examining the connection between backwater flow and sediment transport. The Empire survey conducted in the backwater lowermost Mississippi River shows sediment discharge increased by 100-fold with a four-fold water discharge (Nittrouer 2011). Since backwater flow is prevalent in all coastal river systems, seasonally varying river discharge, as seen in the Carmel River, gives rise to seasonally varying sediment movement and beach metamorphosis (Figure 2).

Overall, the Carmel River breaching system has consistently maintained its physiognomies when observed over long periods, though breach locations occasionally migrate meridionally by hundreds of meters throughout the breaching season (James 2005). Despite expected beach erosion due to consistent offshore sediment transport (from breaching) and migration the morphological stability infers that studies analyzing small

temporal samples are acceptable and studies encompassing longer sample periods are not necessary when assessing sediment transport characteristics. The Rich and Keller geomorphic model used to better understand the hydrography of bar-built estuaries showed longer breaches are due to river discharge and streamflow (Rich and Keller 2013). Accretion and erosion of displaced sediment during breaching leads to unpredictable beach transformations and significant issues with transportation infrastructure and surrounding homes, despite the long-term beach stability.

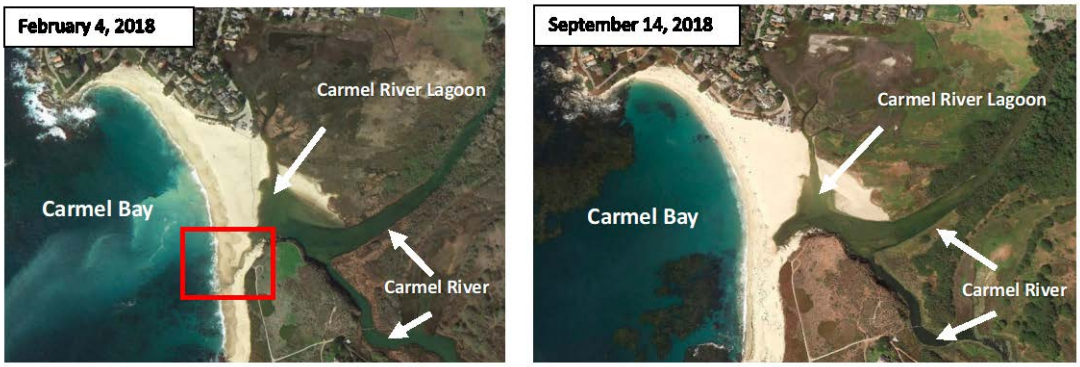

Winter Carmel River breach, occurring in February, outlined in red. These images were generated using Google Earth.

Figure 2. Carmel River State Beach Aerial View

This study examines velocity profiles of various locations in a breaching event at the Carmel River on March 5, 2020, and the berm elevations leading up to and immediately after the breach. Though there have been observed thresholds that, when met, typically lead to breaching or closing of the lagoon, the evolution of velocity profiles and rates/quantities of morphological evolution during a breach are unknown. In-situ water flow measurements collected by transecting the breached river can assist in building velocity profiles and quantify sediment transport potential in efforts to gain clarity of the long-term sediment transport. Water flow velocities should be proportional to sediment transport rates yielding the hypotheses that river discharge rates and momentum fluxes establish sediment transport rates and sediment accretion rates are larger on areas of underpredicted and unstable berm elevation.

III. METHODOLOGY

In order to address the hypotheses that 1) river discharge rates compared to momentum fluxes establish discharge velocities during a breach, and 2) sediment accretion rates are larger on areas where the berm is unstable, observations of berm elevation and breach geometry, as well as discharge measurements, were made at Carmel River State Beach between February 14 and March 9, 2020. These observations spanned several breach events, while this study focused on morphological response around the March 5 breach.

A. FIELDWORK AND DATA COLLECTION

All breach flow and bathymetry data from this study were collected during the March 5, 2020, breach. To measure in-situ breach characteristics the SonTek RiverSurveyor M9 nine-beam, multi-frequency acoustic Doppler profiler (ADP) was used (Figure 3). Transecting the river, an ADP is capable of measuring evolving properties of the breach including mean water column velocity, water velocities throughout the water column, river discharge rates, and bathymetric measurements of the evolving riverbed.

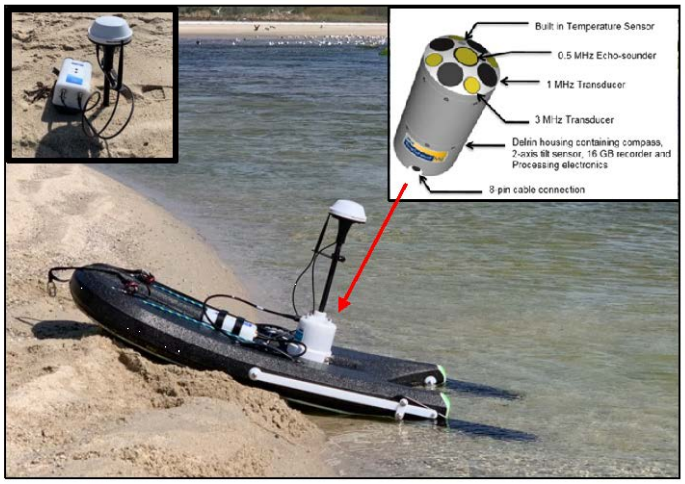

This is a photograph of the SonTek RiverSurveyor installed in the SonTek Hydroboard II along with the mobile real-time kinematic (RTK) GPS station in the Carmel River. The photograph in the top left corner is a photograph of the RTK GPS base station. The image in the top right corner is the ADP depicting placement of the transducers, echosounder, and temperature sensors (SonTek, a Xylem, brand RiverSurveyor S5/M9 System Manual).

Figure 3. SonTek RiverSurveyor M9 Acoustic Doppler Profiler

With the ADP installed, the SonTek Hydroboard II was manually towed across the breached river at ten different locations (Figure 4). In order to observe adequate flow measurements, the locations were in areas where the water flow seemed to be the most turbulent, yet the Hydroboard was able to freely traverse the water with no obstructions and with adequate depth for accurate calculations. The first location was sampled twice, once at the beginning of surveying and once at the end of surveying, to show the transformation of the river from start to finish of the data collection period. A real-time kinematic (RTK) GPS base station was positioned on the beach in a direct line of sight of the RTK GPS station mounted on the ADP and provided precise position data during data collection.

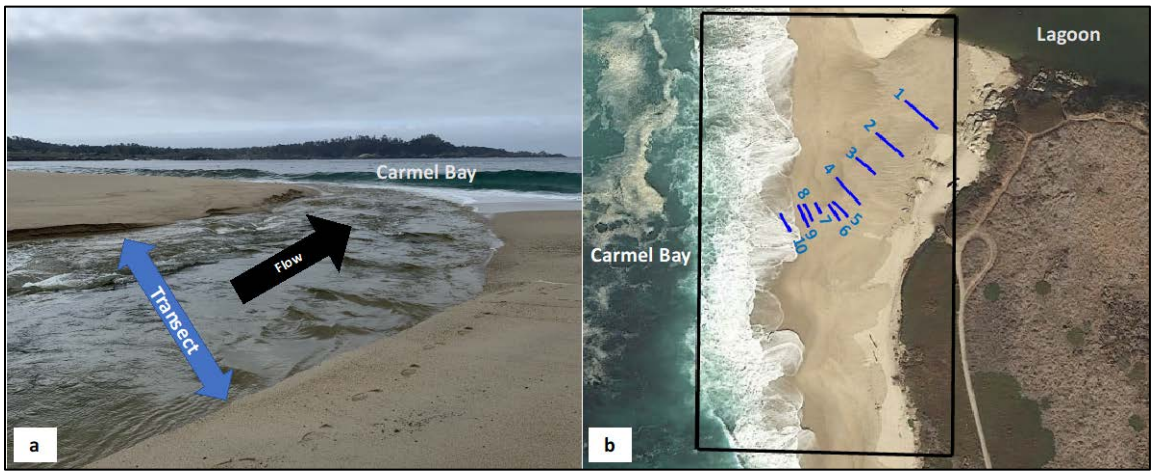

The image a was taken during the March 5, 2020 breach and depicts the orientation of a transect relative to the breached river. Shown in image b are the ten transect locations and total survey area plotted on a November 2018 satellite image, when the river was closed. This image was generated using Google Earth.

Figure 4. ADP Transects

All beach berm elevation data were collected on various dates between February 14, 2020, and March 9, 2020, using the Spectra Geospatial SP60 Global Navigation Satellite System (GNSS) receiver (Figure 5). The SP60 receiver was attached to a mobile backpack apparatus allowing hands-free walking surveys to be completed traversing large parts of the beach based on the beach morphology and river placement that day.

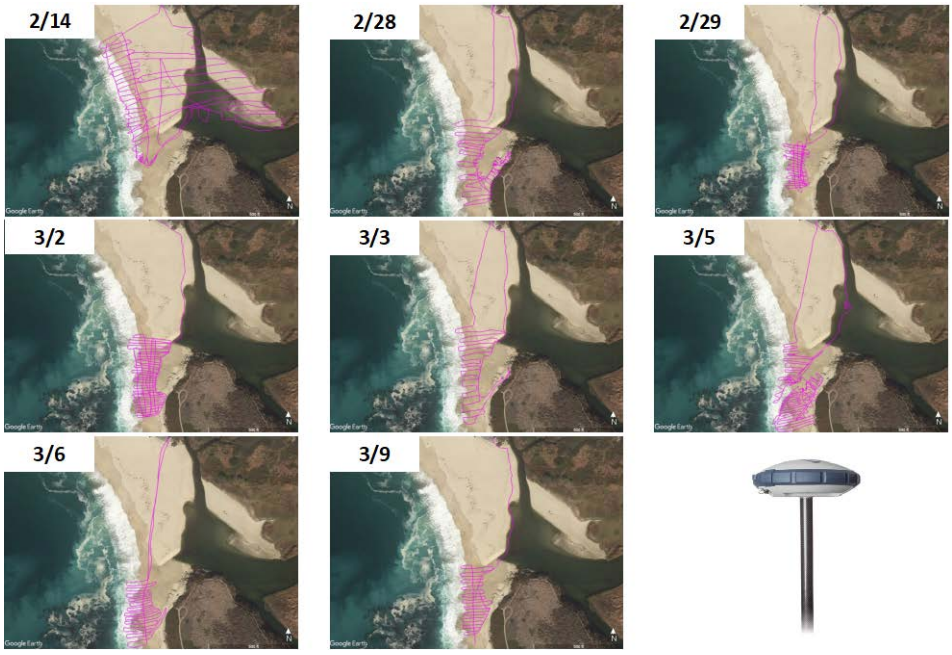

The GNSS receiver and the GPS paths take during each survey. These images were generated using Google Earth.

Figure 5. GNSS Receiver and GPS Walking Survey Paths

B. DATA ANALYSIS

1. River Surveyor

The *RiverSurveyor Live* software is the measurement interface for the ADP. Owing to operating depth limitations and sediment caused data contamination, the software uses velocity profile extrapolation to estimate the transect start edge, end edge, top transect, and bottom transect. Velocity profile extrapolation uses a power law (Equation 1) to approximate velocities around measured velocities

$$\frac{u}{u_*} = 9.5 \cdot \left(\frac{z}{z_0}\right)^b, \quad (1)$$

where u is velocity at height z measured at the river bottom, u_* is bottom shear velocity, z_0 is bottom roughness height, and b is a constant (b=1/6), (Chin 1991).

The ADP measures the middle of the transect (Figure 6). Total discharge and velocities are the summation of the middle measurements, extrapolations, depth, and movement of the ADP as it transects (SonTek Manual).

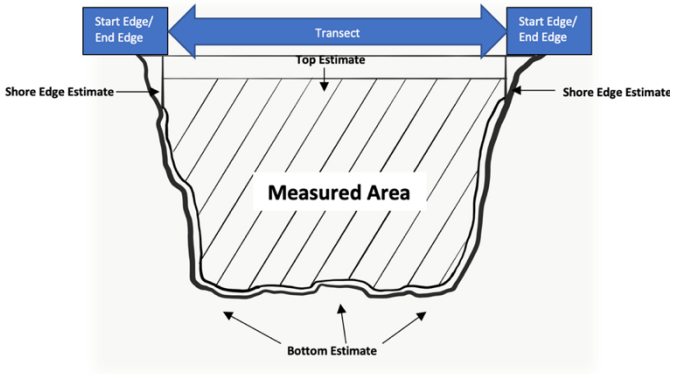

Figure 6. Cross Section of ADP Data Collection Transect Area. Adapted from SonTek, a Xylem, brand RiverSurveyor S5/M9 System Manual.

SmartPulseHD™ feature allowed a wide range of conditions to be analyzed by the RiverSurveyor without preset inputs. Based on tracked water velocities and depths, the ADP selects optimum processing configuration by sending multiple pulse types and utilizing various processing techniques. The cell size adjusts with varying depths (Figure 7).

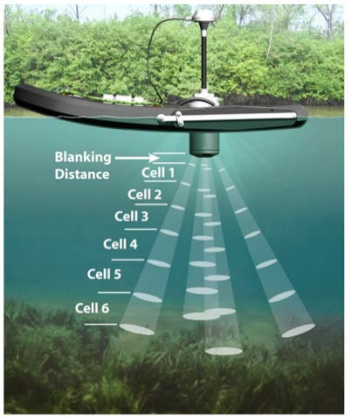

Figure 7. RiverSurveyor SmarPulse™ adjustable cells. Source: SonTek, a Xylem, brand RiverSurveyor S5/M9 System Manual.

The ADP collects river characteristics with three frequencies: 0.5 MHz, 1 MHz, and 3 MHz. Precise velocity profiles are measured by the 1 and 3 MHz transducers, which deliver acoustic pulses and use the Doppler shift principle to measure water velocity in the water column. The speed of the ADP through the water is calculated using GGA GPS reference velocity protocol, applying the collected RTK GPS data, to reduce positional error. In conjunction with doppler shift from multiple acoustic pulses, the ADP is able to deduce vessel speed through the water as well as the speed of the water. The 0.5 MHz echosounder measures depth to illustrate bathymetric characteristics of the riverbed.

2. GPS Surveys

GPS location and elevation data were collected by the SP60 on February 14, 28, and 29, and March 2, 3, 5, 6, and 9 (Figure 5). Referencing UTM coordinates, the survey area was 100x170 meters and interpolated onto a mesh grid with 100 grid points in both x and y-directions, approximately one grid point per meter in the x-direction and 1.7 meters in the y-direction. Elevation data was corrected using measured antenna height above ground for each survey. The default system output for SP60 elevation utilizes the WGS84 ellipsoid as a reference point. During data processing, it was corrected to reference the NAVD88 mean sea level datum utilizing the system's GPS undulation calculation. The ADP system has both NAVD88 and WGS84 elevation outputs. For continuity, the WGS84 ellipsoid ADP output was used and corrected with the same SP60 system undulation used for the SP60 elevation. Ultimately, both the SP60 elevation and the ADP bathymetry data referenced NAVD88 datum for z-direction calculations.

For the berm elevation calculations, the SP60 used of all six GNSS systems for precise positioning: GPS, GLONASS, BeiDou, Galileo, QZSS and SBAS. This provides the flexibility for SP60 to operate in GPS-only, GLONASS-only or BeiDouonly, which makes the SP60 optimal for tracking and processing signals.

During data assimilation from each survey, overall elevations changes were compared as well as cross-shore and longshore maximums and minimums. This sampling technique accurately depicted accretion and erosion extremes while creating an outline for calculation sediment mobility and fluxes.

THIS PAGE INTENTIONALLY LEFT BLANK

IV. RESULTS

A. BREACHING AND CLOSING EVENTS

The river breached several times during morphological data collection, as evidenced by rapid drops in water levels (figure 8b). During this time, winter offshore waves were between 2-4m offshore (Figure 8a). Since it was not possible to directly observe each breach, it was necessary determine when the breaches occurred in order to evaluate resulting elevation affects. Using momentum balance estimates (Orescanin and Scooler, 2018), where dynamic pressure between river discharge and ocean waves and tides are evaluated, the temporal element of relative ocean and river momentum fluxes are able to be determined (Figure 8c). When water levels in the lagoon exceed the berm minimum elevation, a breach occurs, and the river remains open. When river discharge and ocean forcing processes are equal or ocean forcing dominates, the river will close (Figure 8c). In contrast, if river discharge dominates (after March 15, Figure 8c), the river will remain open. Given, MPWMD river discharge measurements, lagoon water levels, and offshore tidal information it was possible to determine the Carmel River breach and closure cycles for this survey time (green areas, Figure 8b, Table 1). This was established by flagging times where the water level difference between the lagoon and the ocean was larger than one standard deviation above the mean ocean water level. Prior to February 20, the river went through nearly daily partial closures, when river discharge levels were low relative to ocean forcing (Figure 8c), similar to the effects seen at other systems with a well-established sediment sill (Williams and Stacey 2015). Between February 20, and March 13, the river had four periods of longer term (>tidal cycle) closures, including the breach on March 5th (the focus of this study), before finally opening on March 15th. Prior to the March 5th breach, the beach remained closed for five days, leading to beach berm growth and water level increases (Figure 8b-c)

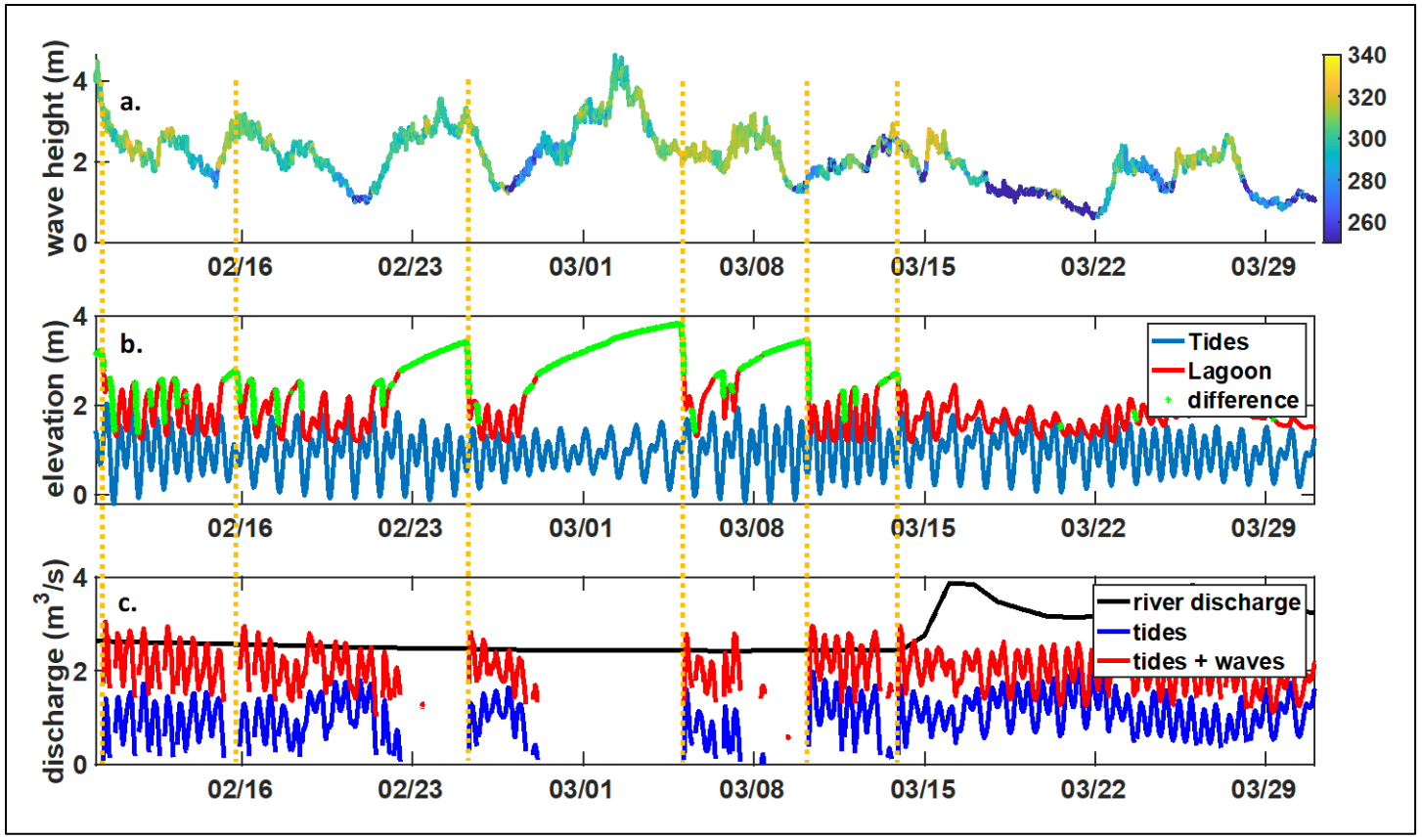

a. Time series of offshore wave heights colored by wave direction. b. Water levels in the lagoon and tides. Breaches and closures for more than one tidal cycle are indicated by orange dotted lines. c. tides and waves, river discharge, and tidal activity.

Figure 8. Carmel River State Beach Momentum Balance for Breach/Closure

Table 1. Carmel River Breach and Closure Dates

River Open (Breached)	River Closed
February 10	February 15
February 15	February 22
February 25	February 28
March 5	March 7
March 10	March 13

B. ELEVATION TRANSFORMATIONS

The GPS surveys conducted with the SP60 show elevation variations relative to NAVD88 between February 14, 2020 and March 9, 2020 (Figure 9). During the February 14 survey, the river was experiencing a breaching cycle where the river was connected to the bay. The breach opened on February 10 and closed on February 15 allowing only the north portion of the beach to be surveyed. The river briefly closed on the morning of the 15th only to reopen later in the evening until the 22nd. A breach occurred on February 25 as well, leaving the river open to the bay until February 28. Morphological observations were made with an overall accretion of sediment (~0.25-1.5m) between the February 14 (Figure 9a) and February 28 (Figure 9b) surveys on the north side of the beach (Figure 10a). Since there was no continuous build-up of sediment by waves between the 14 and 28 surveys due to the breaching cycle (the river was intermittently open, and breached two times), the berm fluctuations are not as drastic as would have been expected because the beach berm had to rebuild twice during that time period. The survey on February 29th shows an overall gain of sediment from the February 28th survey (~0.25-0.5m) although the northern western portion of the survey appear to show significant erosion (~1.0-1.5m), likely owing to the survey on February 29 not fully mapping the northern extent (Figure 5 Figure10b). The enduring accretion on surveys from February 29 to March 3 (Figure 10c and 10d) is especially evident on the beach face as well as the back-beach (~0.25-1.5m). Once the river breach occurs on March 5, sediment is displaced and eroded to the ocean,

minimizing elevations within the river, back-beach, and along the river's edge (~1.0-1.5m)) though along the beach face sediment is building (~0.25-1.0m) (Figure 10e). The survey taken on March 6 shows the sediment build up beginning to occur as the river fights the pressure on the oceanside to stay open (~0.25-1.5) (Figure 10f). The river is overcome by the pressure gradient and the momentum balance is stabilized on March 7. The survey on March 9 shows the sediment accumulation especially within the river (~0.25-1.5m) leading up to the next breach on March 10 (Figure 10g).

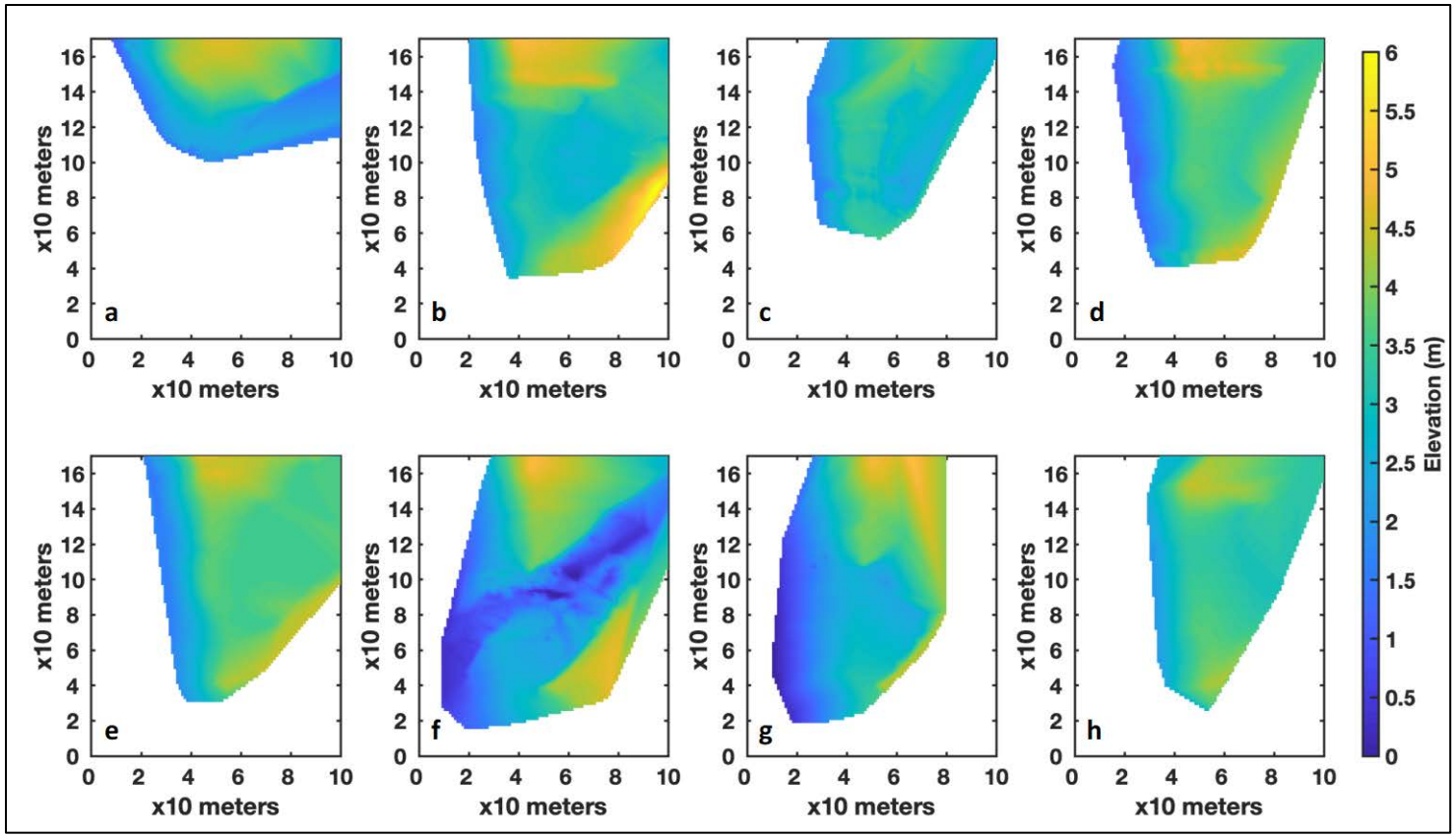

a. February 14 b. February 28 c. February 29 d. March 2 e. March 3 f. March 5 g. March 6 h. March 9. Plots made with a combination of SP60 GPS and ADP bathymetry data. Survey area 100 by 160 m (Figure 4). All elevations reference NAVD88.

Figure 9. Elevation Plots of Carmel River State Beach Surveys

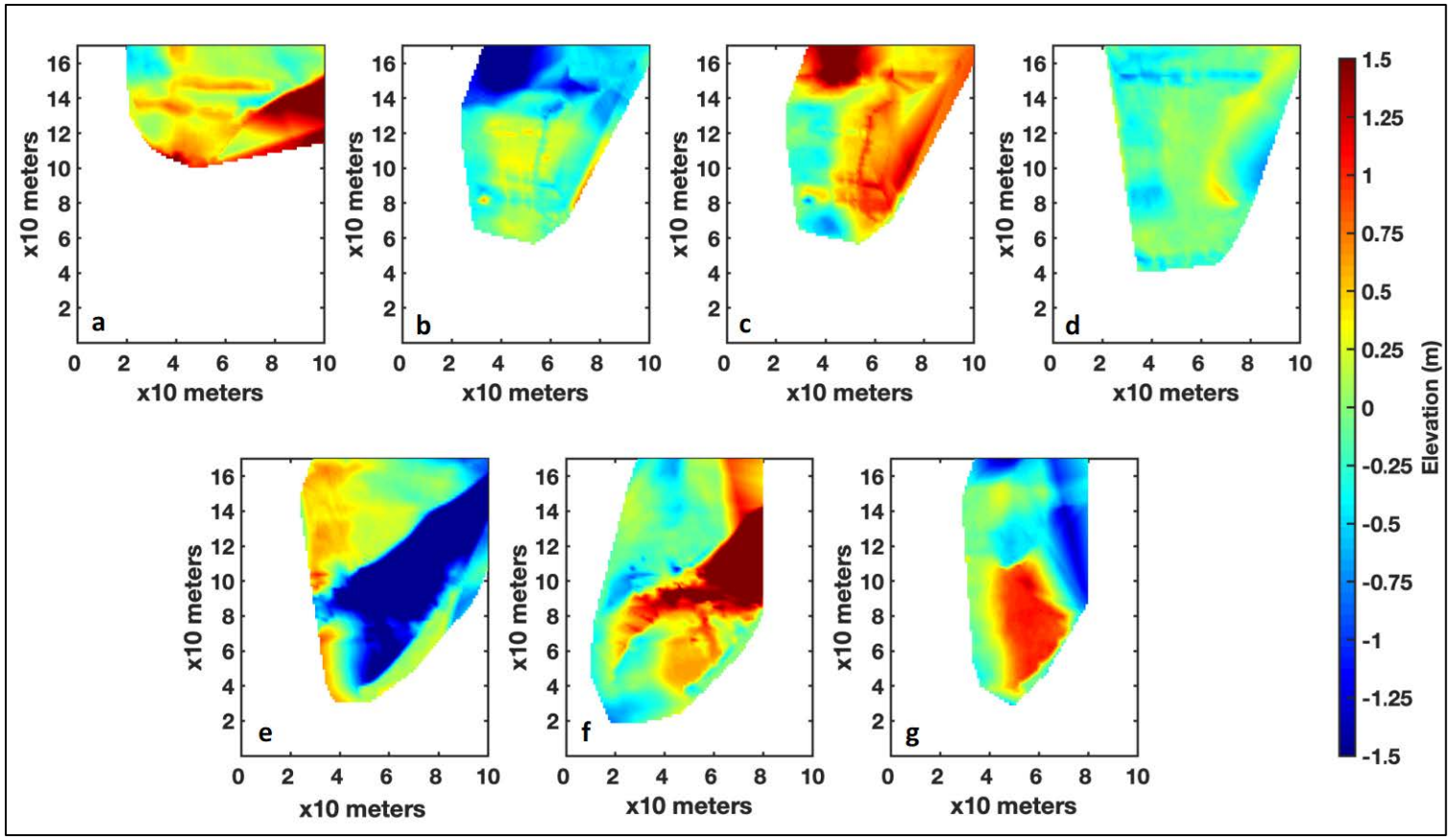

a. February 14 vs. February 28 b. February 28 vs. February 29 c. February 29 vs. March 2 d. March 2 vs. March 3 e. March 3 vs. March 5 f. March 5 vs. March 6 g. March 6 vs. March 9. Plots made with a combination of SP60 and ADP data. All elevations reference NAVD88.

Figure 10. Elevation Difference Plots of Carmel River State Beach Survey

Quantifying longshore berm evolution, the beach was evaluated in three sections: front-beach (transect 1, Figure 11a), mid beach (transects 2 and 3, Figure 11a), and back-beach (transect 4, Figure11a). Quantifying cross-shore berm evolution, beach surveys were evaluated in three sections: North (transect 1, Figure 11b), In-Channel (transects 2 and 3, Figure 11b), and South (transect 4, Figure 11b). Transects 2 and 3 for cross-shore profiles are combined to accommodate the location of the channel during the observed breach on March 5th.

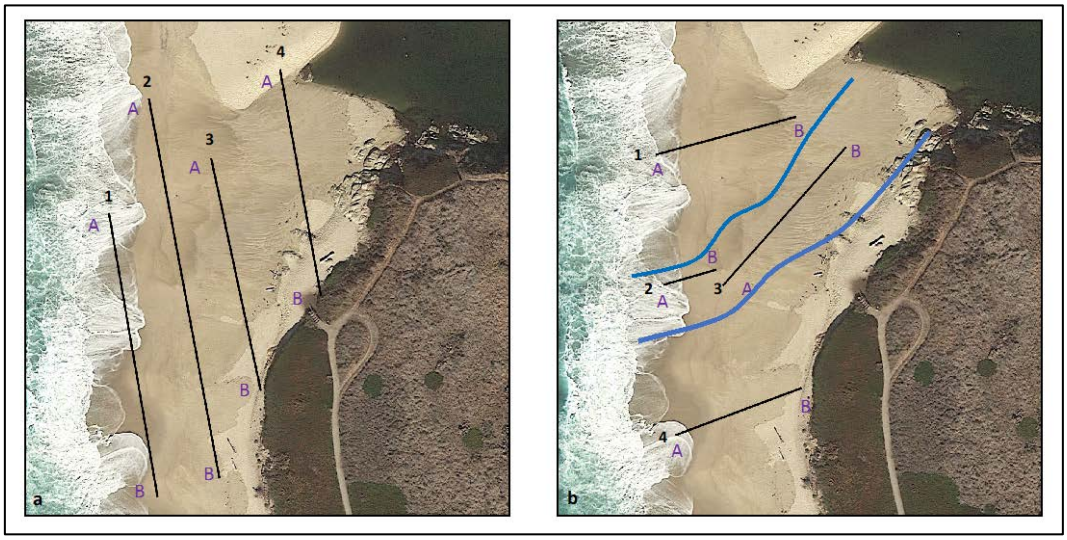

a. Longshore samples: sections 1 (94m) referred to as front-beach, sections 2 (126m) and 3 (78m) are mid-beach, and section 4 is back-beach. b. Cross-shore samples with an estimated outline of the March 5 breached river: section 1 (46.5m) is North, sections 2 (17.5m) and 3 (59m) are In-channel, and section 4 (43m) is south. Images provided by Google Earth.

Figure 11. Longshore and Cross-Shore Sampling Schematic.

1. Longshore

The longshore transects show distinct elevation differences created by the breaching river (Figure 12a-d). The river channel outline is depicted in the surveys collected during breaching events (black lines, Figure12a-d). In general, the longshore surveys suggest higher elevations with less variance along the southern part (B locations, Figures 11a, 12a-d). In order to assess the required water level for overtopping at each longshore transect, the minimum elevations were extracted and compared between surveys

(Figure 13). Prior to the March 5 breach, the minimum elevations increase for all transects, suggesting net accretion, but increase most along the berm crest and behind (transects 2-4, red, yellow, and purple lines, Figure 13). After the March 5 breach, the recovery of the beach is immediate (within 1 day).

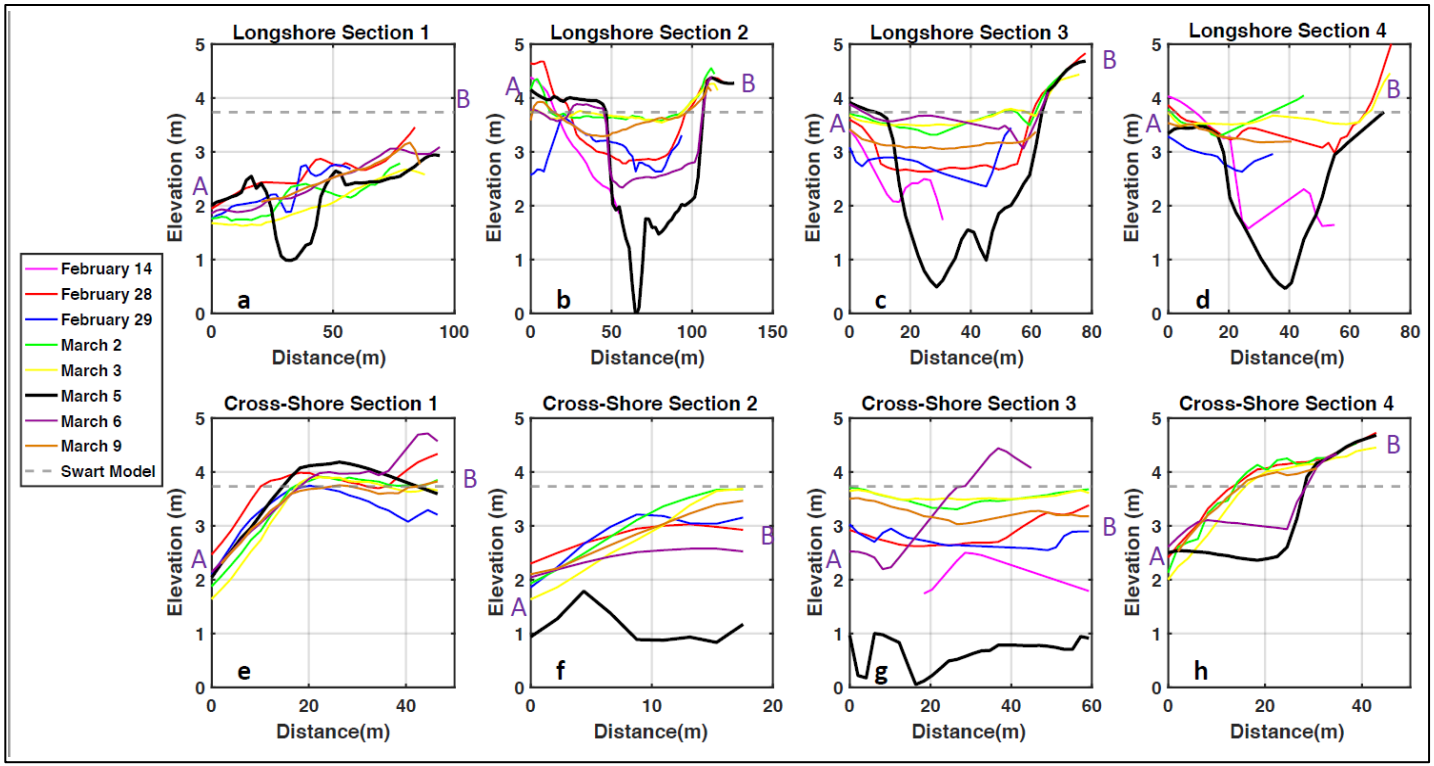

Cross-shore and longshore elevations extracted from Figure 11. a. Longshore Section 1, b. Longshore Section 2 c. Longshore Section 3 d. Longshore Section 4 e. Cross-Shore Section 1 f. Cross-Shore Section 2 g. Cross-Shore Section 3 h. Cross-Shore Section 4. Swart model calculated using Swart 1974 Berm estimate model. All elevations are relative to NAVD88.

Figure 12. Longshore and Cross-Shore Survey Samples

a. Front-Beach

During the active breaching, longshore transect 1 (black line, Figure 12a) shows channel edge elevations that are the lowest, compared to other regions of the breach channel (black line, Figures 12b-d and blue line, Figure 13), of the survey while the lowermost river channel elevation, i.e. the thalweg, is the highest suggesting the presence of a roughly 1m sill separating the upstream channel (transects 2-4) from the ocean. This is the closest survey sample in proximity to the Carmel Bay making it experience the most ocean wave (swash) and tidal energy, which promotes channel closure and sediment accumulation more than a back-beach location. It is therefore, not unexpected that there is no distinct trend in accretion or erosion along this transect throughout the other survey dates, as it is more likely to change owing to varying offshore wave heights.

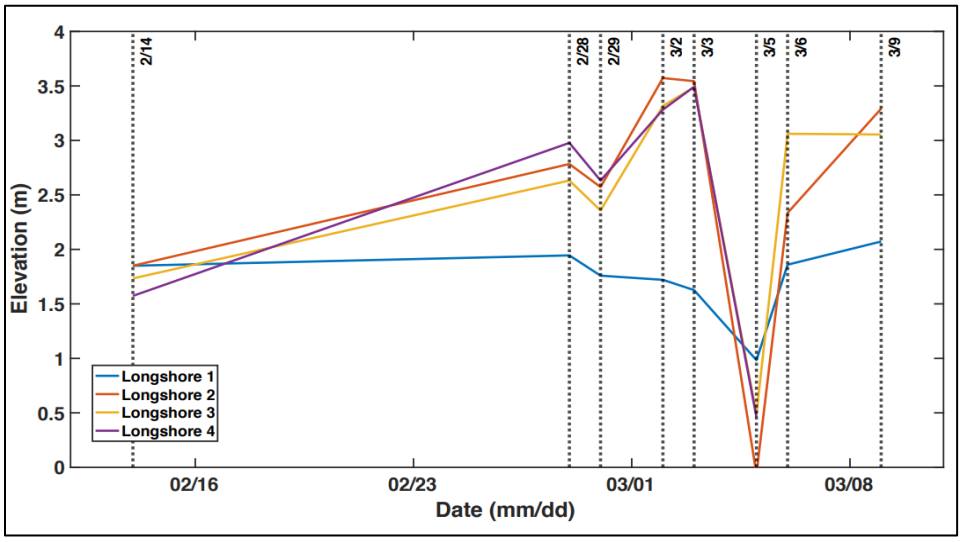

The minimum elevation measured each sampling day for longshore sections 1-4 from Figure 12a-12d

Figure 13. Longshore Minimums

b. Mid-beach

In longshore transects 2 and 3 the same steady accretion of sediment can be observed between the Feb 28 closure and March 5 breach by looking at the elevation differences. For both longshore transects 2 and 3, there is a net accretion in both locations leading up to the breach on March 5. The immediate erosion of roughly 4m in the channel thalweg occurs during the early stages of breaching, where the deepest part of the channel is along transect 2. After closure, there is again a recovery of the beach, with accretion approaching the pre-March 5 levels. As these locations represent possible minimum elevations required for overtopping, the minimum values of longshore transects 2 and 3 suggest that after the February 29 survey, the berm begins to rebuild (Figure 13). On March 2 and 3 upward sediment development continues until the river breaches on March 5. Beginning February 29, wave and tidal energy strongly oppose the river discharge (Figure 8c) leading to berm accretion until energy exiting the channel surmounts energy entering the channel on March 5 causing the breach.

c. Back-Beach

Berm evolutions on longshore transect 4 are similar to the mid-beach berm evolutions (Figure 12d, Figure 13). This shows the influence of the ocean forcing energy signal during the February 14 to February 28 closure by the accretion levels of over a meter in the channel.

2. Cross-Shore

The north (cross-shore transect 1, Figure 11b), in-channel (cross-shore transects 2 and 3, Figure 11b), and south (cross-shore transect 4, Figure 11b) transects show the evolution of the cross-shore beach faces and river channel, showing the development and deterioration of the river sill with breaching cycles.

a. North

As seen in the long shore samples, cross-shore section 1 (Figure 12e) elevations decay after the February 28 closure, with a net loss of approximately 0.5m from the face of the beach by the March 5 survey. During that survey sediment levels are higher than

levels measured just before the breach on March 2 and 3. March 6 and 9 surveys stay just below the March 5 levels. As for the back-beach measurements after the closure on the 28th, the beach experiences a brief decline on the 29th then starts to rebuild beyond the breach until the closure on the March 7. Overall, there is not a significant profile change in the north cross-section 1, but small (<.25m) accretion or erosion offsets between surveys, especially on the beach face.

b. In-Channel

Owing to the shape of the channel, cross-shore transects are split into two sections, which, when combined, show the cross-shore profile of the channel thalweg (Figure 11b). Cross-shore section 2 (Figure 12f) shows the evolution of the river channel near the sill. After the February 28 closure, a well-defined sand sill begins to build and migrate up the beach as the oceanside energy overcomes the river discharge pressure. However, river discharge in the lagoon ultimately fills the water levels above this sill height, leading to the March 5 breach. After the breach, the March 6 sill develops and by March 9 migrates inward as the ocean energy overcomes the discharge forces again, bringing in sediment through wave overtopping processes (Figure 8c). When the river is closed and waves are able to overtop the sill, sediment builds and is able maintain the pressure gradient between the river and lagoon and ocean until a breach occurs (Figure 14). The ocean forced March 6 sill migrates into the channel with the propagated ocean energy and subsiding river discharge, and partially blocks the channel from the lagoon. The sill protrusion is diminished on March 9 after the river has closed.

When the sand sill at the breaching location is able to build elevation above the water level in the lagoon, the sill remains intact. However, if these water levels exceed the sill elevation, then breaching occurs by overtopping from the lagoon side (Compare red/yellow markers with blue elevation line). Visual observations made during the March 3 survey indicated water levels were within ~20cm between the lagoon and max sill elevation (not shown).

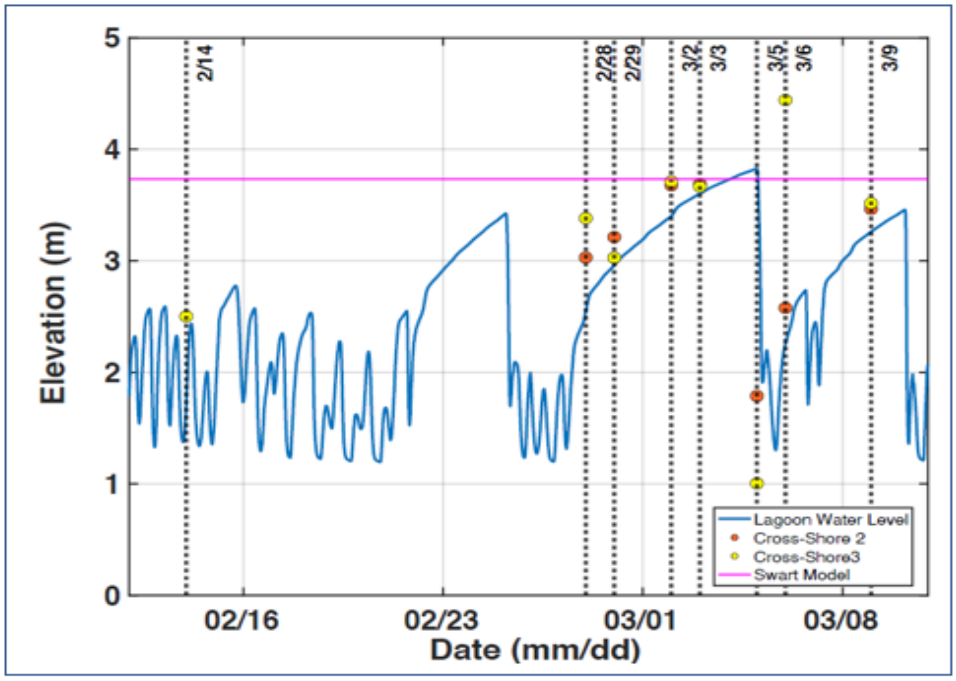

Lagoon water levels reported by MPWMD. Swart 1974 model estimates berm crest elevation based on sediment transport by wave action. All elevations are in reference to NAVD88.

Figure 14. Lagoon Water Levels, In-Channel Maximums, and Swart Model Berm Estimate

c. South

Cross-shore section 3 is comparable the North beach survey. Leading-up to the March 5 breach, the beach front builds slightly (<0.1m) and maintains its shape. During the breach the beach face shows significant loss in elevation until the river is closed again. Recovery from the March 5 breach occurs by March 9 along this portion of the beach. It should be noted that the south side of the beach is flanked by rocky outcrops, limiting any possibility of wave overtopping.

C. EMPIRICAL BERM HEIGHT ESTIMATES

A relationship between the maximum recorded berm and oceanside energy or wave run-up can be established using the Swart 1974 model.

$$Bc = D50\ (7644 - 7706e^{-A})$$

where

$$A = 0.000143\ (H_0{}^{0.488}\ Tp^{\ 0.93})/(\ D_{50}{}^{0.786})$$

and D_{50} is average grain size of sediment present in berm, 0.06m cobble and 0.002m sand, H_0 is deep water significant wave height, 2m, and T_p is peak wave period, 13s. The values used for this estimation are from average values from the Point Sur NDBC buoy (wave heights shown in Figure 8a). Grain size samples were taken over several locations at various times throughout the season and yielded a highly variable sediment composition. However, while thin gravel to cobble sized layers existed, the majority of sediment available is classified as coarse sand, with D_{50}= 0.65-2.0mm his model is based on the connection between the median sediment grain size and beach face slope (Swart 1974, Booysen, 2017). Swart's Model helps predict the berm elevation (B_c) prior to a breach given oceanside factors and sediment composition. Figure 12 compares the berm measurements surrounding the March 5 breach and quantifies the effects of the riverside forces.

D. BREACH VELOCITY PROFILES

Of the ten transects made to measure water velocities, bathymetry, and river discharge in the channel during the March 5 breach, three longshore samples were selected to represent the velocity data collected: transects 1, 4, and 6 (Figure 4). These three samples encompassed what was observed in their respective longshore locations: front-beach, mid-beach, and back-beach (Figure 15).

For transects landward of the channel bend (transects 1-4), river velocity measurements taken on this part of the back-beach have an overall uniformed magnitude flow throughout the water column. Speeds at the surface are similar to the speeds at the bottom (~0.2-0.4 m/s). For all the transects, the fastest speeds are on the north side of the flow and slower speeds that appear to reverse back into the channel on the southside. Mid-beach measurements are more of a uniformed flow throughout the channel (~0.2-0.5 m/s). Although there is a slight northerly increase (~0.1-0.2 m/s) on the northside of the flow. The front-beach velocity measurements are the most turbulent (Transect 6, Figure 15).

They have distinct depth variations with sporadic changes in northernly and easterly contributions. The highest velocities were observed in the front-beach measurements (~0.5-1 m/s). This is consistent with visual observations that this was where the channel abruptly changed orientation owing to bedrock constrictions along the south side of the channel. While the channel is relatively short, there is substantial horizontal flow structure, especially near the bedrock constriction at transect 6. The stronger velocity magnitudes along the northern side of Transect 6 are consistent with observations that the channel edge was actively eroding during data collection.

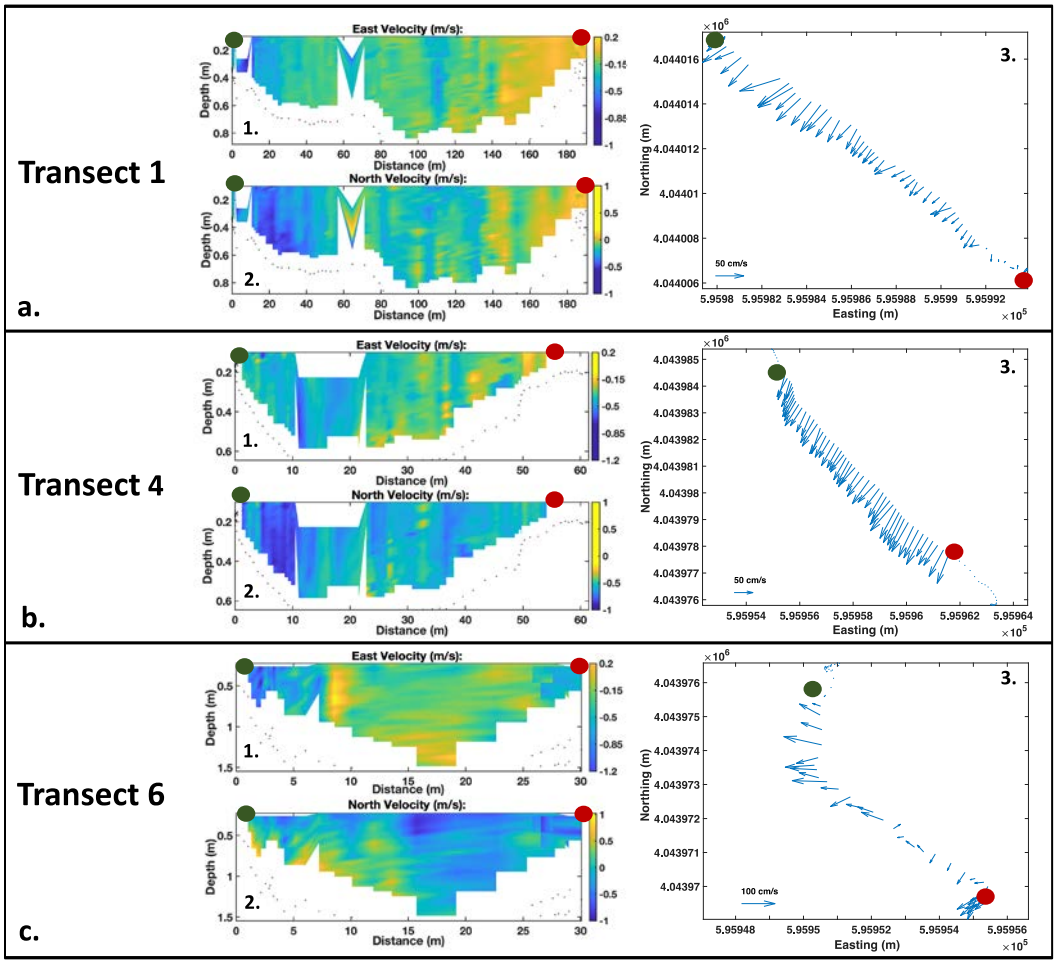

a. Transect 1: Front-beach, b. Transect 4: Mid-beach, and c. Transect 6: Back-beach. Reference Figure 4 for transect locations. The start of the transect is at the green dot and the end of the transect is at the red dot. East and North vertical sections of velocities are measured from the top of the water to the river bottom (a1,a2,b1,b2,c1,and c2). Vectors are mean velocity of the water column (a3,b3 and c3).

Figure 15. ADP Velocity Measurements during the March 5 Breach

Total discharge rates at transects 1,4, and 6 average 1.95 m^3/s (Table 2). Daily mean average discharge at the Highway 1 basin streamflow gaging station of Carmel River (Figure 16) on March 5 was 1.08 m^3/s. This is consistent with the momentum balance formulation that owing to storage capacity within the lagoon, additional discharge may occur through the breach channel owing to the pressure gradient between the lagoon and ocean combined with the river discharge (adding river discharge to tidal forcing without waves, Figure 8c). The discharge at and around transect 4 at the beginning of data collection was 2.02m^3/s. After all samples were collected it was 2.12 m^3/s.

Red circle around the Carmel River Highway 1 bridge streamflow gage operated by MPWMD approximately1km upstream. Image provide by Google Earth.

Figure 16. Upstream Measurement of Carmel River

Table 2. Carmel River Discharge March 5, 2020

Measured Location	Highway 1	Transect 1	Transect 4	Transect 6	Expected (momentum balance)
Rate (m^3/s)	1.08	2.23	2.02	1.95	1.85

Transect rates measured during March 5 breach. Highway 1 measurement is from the Carmel River Highway 1 bridge daily mean average March 5, 2020 done by MPWMD.

V. DISCUSSION

A. SEDIMENT MOVEMENT AND BERM STABILITY

The progressive accretion and erosion of the beach sill during, leading up to, and immediately following numerous winter breaches at Carmel River State Beach are shown through repeated surveys of morphology. When oceanside energy is dominant, the river closes and when the river discharge is great, causing elevated water levels in the lagoon, a breach occurs (Rich and Keller 2013, Orescanin and Scooler 2018). During the sampling period the river closure signal, shown when tides and wave energy are equal and opposite the river discharge energy (Figure 8c), display a well-defined response exhibited where a low berm becomes a now distinct barrier. The location of the sediment as the wave energy continues to dominate and percolate up the river, is mimicked with the sill migration inland (Figure 12e and 12f). When wave energy is dominant, sediment elevation builds. This is consistent with findings of Rich and Keller (2013) and Behrens et. al (2013).

The berm evolution is not exclusive to the river mouth location. There was noticeable berm fluctuation immediately to the north and south of the breach coinciding with the signal response seen upstream with increased oceanside energy. When the oceanside forces are dominant, the berm grows in these locations as well. The mobilized sediment in Figure 12e and 12h as well as the A and B (beginning and end) points in all of the longshore sections in figure 12a -12d show this build-up, though not at the rates seen in the river channel.

The expected berm elevation of a barrier beach has been estimated previously based on offshore wave climate and sediment characteristics (Swart 1974, Booysen 2017). The Swart model can be used to predict berm growth based on observations during the data collection period. When the measured berm is comparable to the modeled height, the berm is displaying stable predictable morphology. When it is varying, the berm is showing signs that the sediment transport is more susceptible to effects of the momentum flux between ocean and river forces. The most instability is seen in the channel where the most

momentum flux is seen (Figure12 and 13). It is also seen in the areas in close proximity to the ocean (Figure12a).

B. RIVER DISCHARGE VS. TIDAL AND WAVE ENERGY

During the March 5 breach average measured river discharge was, 2.07 m^3/s, whereas the river discharge was 1.08 m^3/s at the Highway 1 bridge. The average daily discharge (Figure 8c) stayed consistent through the entire sampling period whereas ocean and tide discharge varied throughout the sample period (Figure 8c). That implies the river discharge driven sediment load stayed the same while the oceanside increased and decreased leading to closures and breaches. The ocean energy was the dominating contributing factor to the river breaching and closing cycles during the observation period. This is apparent in Figure 12 primarily during the cross-shore sediment transport instances. The sills can be seen moving with the wave energy up-river. When the wave energy subsides, the sediment moves with the river discharge causing a breach.

ADP measured river velocities on March 5 at the mouth of the river are the highest and most turbulent. When comparing accretion and erosion March 3-6, the river opening to the ocean is where the most elevation difference and sediment movement was observed (Figure 10e and 10f). This shows a correlation between river flow velocities and sediment transport of the submerged sill, as seen in Orescanin and Scooler (2018) expected velocities.

While the measured river discharge was 2.07m^3/s, the expected flow rate on March 5 based on river vs. ocean forces (momentum balance) was 1.85m^3/s. In order to remain open, it has been shown that, with Carmel River's wave climate, discharge rates typically must exceed 5.5m^3/s (James 2005). During the sampled period, the discharge rate was less than that during breaches. In these instances, oceanside activity contributes to the active breach time (Rich and Keller 2013, Orescanin and Scooler 2018).

VI. CONCLUSION

Carmel River is an ephemeral river with a breaching and closing cycle dependent on the direct pressure gradient established between river (lagoon) discharge and ocean forced energy. These dynamic hydro-physical properties contribute to the evolving morphology and sediment displacement at the beach especially during the winter months. Examining evolving sediment elevations, momentum flux between the river and oceans, and in situ breached river velocities, this study was able to make inferences with regards to possible contributions to dynamic morphological characteristics.

GPS walking surveys were conducted surrounding the March 5 breach between February 14 and March 9. Ocean wave and tidal data as well as velocity (discharge) measurements were analyzed to help explain morphological contributions at a breach and how quickly they can accrete and erode sediment. The study was able to observe the instability around a breaching channel. The stability of the morphology of the channel is heavily reliant upon hydraulic forces. Sediment accretion and erosion respond to the river and ocean signals. An Ocean driven sediment load can be seen when the ocean has the most dominant energy, this presents itself as an oceanside sediment build up or sill within the channel. Conversely, when the river energy is dominant, the river channel sediment erodes making way for the river to connect to the ocean. Where river velocities (discharge) were the greatest, the most erosion was observed.

Follow-on work at Carmel River could include measuring actual sediment transport rates as they related to ocean wave overtopping vs. tidal activity. During this study, there were too many contributing factors between survey periods that would not allow an accurate rate calculation. In the assessment of future breaches, determining the effect of breach migrations on beach stability and overall morphology could be evaluated as well.

THIS PAGE INTENTIONALLY LEFT BLANK

LIST OF REFERENCES

Behrens, D. K., Bombardelli, F. A., Largier, J. L., and Twohy, E., 2013: Episodic closure of the tidal inlet at the mouth of the Russian River—A small bar-built estuary in California. *Geomorphology*, **189**, 66–80.

Booysen Z., 2017. Berm Height and Temporary Open/Close Estuaries in South Africa: Analysis and Predictive Methods. M.S. thesis, Department of Civil Engineering, Stellenbosch University, 200pp.

Davidson, M. A., Morris, B. D., and Turner, I. L., 2008. A simple numerical model for inlet sedimentation at intermittently open-closed coastal lagoons. *Cont. Shelf Res.* **29**, 1975–1982.

Donnelly, C., 2008. Coastal overwash: processes and modelling. Ph.D. thesis, Department of Building and Environmental engineering. Lund University, Sweden, 61pp.

FitzGerald, D. A., 1996: Geomorphic variability and morphologic and sedimentologic controls on tidal inlets. *J. of Coast. Res.,* **23**, 47–71.

James, G. W., 2005. Surface water dynamics at the Carmel River Lagoon Water years 1991 through 2005. Monterey Peninsula Water Management Agency, Monterey, Ca.

Kraus, N. C. and Munger, S., 2008. Barrier beach breaching from the lagoon side, with reference to northern California. *Shore & Beach* **76**, 33–43.

Kraus, N. C., Militello, A., and Todoroff, G., 2002. Barrier breaching processes and barrier split breach, Stone Lagoon, California. *Shore & Beach*, **70**.

Kraus, N. C. and T. V. Wamsley, 2003. Coastal Barrier Breaching, Part 1: Overview of Breaching Processes, *ERDC/CHL CHETN-IV-56*, **March 2003**.

Laudier, A. N.,Thornton, E.B., and MacMahan, J.,2011. Measured and modeled wave overtopping on a natural beach. *Coast Engineering* **58** (2001) 815-825.

Lee, J. S. and Julien, P.Y., 2006. Downstream hydraulic geometry of alluvial channels. *Journal of Hydraulic Engineering* **132** (12), 1347–1352.

Nittrouer, J. A., Mohrig, D., and Allison, M. A., 2011a, Punctuated transport of bed materials in the lowermost Mississippi River: *Journal of Geophysical Research-Earth Surface*, 2011-12 Vol **116** F4.

Nittrouer, J. A., Shaw, J., Lamb, M. P., and Mohrig, D., 2012, Spatial and temporal trends for waterflow velocity and bed-material sediment transport in the lower Mississippi River: *Geological Society of America Bulletin*, **March/April 2012**.

Orescanin, M. M. and J. Scooler, 2018: Observations of episodic breaching and closure at an ephemeral river. *Continental Shelf Research*, **166**, 77–82.

Pierce, J. W.,1970: Tidal inlets and washover fans. *The J. of Geol.*, **78 (2**), 230–234.

Rich, A. and E. A. Keller, 2013: A hydrologic and geomorphic model of estuary breaching and closure. *Geomorphology*, **191**, 64–74.

Swart, D. H., 1974. *Offshore sediment transport and equilibrium beach profiles*, TU Delft, Delft University of Technology.

Williams H. F. L., Contrasting styles of hurricane Irene washover sedimentation on three east coast barrier islands: Cape Lookout, North Carolina; Assateague Island, Virginia; and Fire Island, New York. *Geomorphology*, **231**, 182-192.

INITIAL DISTRIBUTION LIST

1. Defense Technical Information Center
   Ft. Belvoir, Virginia

2. Dudley Knox Library
   Naval Postgraduate School
   Monterey, California